TenSy Grid

Tensors for System Analysis of Converter-dominated Power Grids

D 1.1 Hybrid Implicit Multilinear Model Class and Minimal Format

by IWES

Public

Co-funded by
the European Union

About TenSyGrid

The demand for the power grid in Europe is undergoing profound changes due to an increasing number of decentralized feed-in points and the fluctuating supply from renewable energies. This complexity in interactions between power grid components poses a challenge for maintaining system stability. To address this, the European project TenSyGrid is developing a toolbox for direct stability assessment using multilinear models to capture the complex dynamics of power grid components. The objective is to support grid operators in assessing large power grids primarily powered by renewable energy. The toolbox will be compatible with existing commercial software packages to facilitate integration into current workflows.

Project Title	Tensors for System Analysis of Converter-dominated Power Grids
Programme	Horizon Europe - Clean Energy Transition Partnership (CETP)
Project Number	CETP-FP-2023-00138
Project Type	Research-oriented approach (ROA)
Call Module	CM2023-02 Energy system flexibility: renewables production, storage and system integration
Transition Initiative	TRI1 Net-zero emissions energy system
Project Start	01.12.2024
Project Duration	3 years
Coordinator	Fraunhofer IWES
Project Website	`www.tensygrid.eu`

Consortium

About this document

Deliverable Number	D 1.1
Title	Hybrid Implicit Multilinear Model Class and Minimal Format
Work Package	1
Leading Partner	Fraunhofer Institute for Wind Energy Systems
Authors	M. Eng. Christoph Kaufmann Dr. Carlos Cateriano Yáñez Dr. Sarah Casura
Reviewers	Prof. Dr.-Ing. Gerwald Lichtenberg
Version	V1.0
Due Date	30.11.2025
Version Date	28.11.2025
Reviewer Accepted	26.11.2025
WP Leaders Accepted	28.11.2025

Dissemination Level	
PU	Public

Summary

This deliverable describes hybrid implicit multilinear time-invariant models. It describes hybrid implicit multilinear functions. The representation of hybrid implicit multilinear time-invariant models is derived, including the minimal model exchange format. Examples illustrate the use of the hybrid implicit multilinear time-invariant model class.

Contents

List of Figures

List of Tables

1 Introduction

Multilinear functions are a special class of polynomial functions which become linear when all variables except one are held constant. With this special property, they can be used to model multilinear time-invariant (MTI) dynamic systems, [1], as an interesting alternative to linear time-invariant (LTI) or general nonlinear time-invariant (NTI) models. The advantage of MTI modelling is that it can capture relevant nonlinear dynamics, while being structured, which - together with tensor decomposition methods [2] - allows for efficient representations [3]. In addition, multi-linear functions encompass Boolean functions [4], such that hybrid systems containing both continuous and discrete variables can be represented exactly, see Figure 1.1.

Figure 1.1: Classes of functions

An example is a power switch, which can be on or off. Further examples are shown in chapter 5 and in [5]; and a comprehensive list of nonlinearities in power systems is provided in deliverable 3.1 [6]. Approaches to multilinearize power system components are presented in deliverables 2.1 [7] and 3.2 [8].

Hybrid explicit multilinear time-invariant (eMTI) models were introduced in [9] in the context of heating systems. Implicit multilinear time-invariant (iMTI) models were developed in [3] and have the advantage over eMTI models that they are closed under composition, i.e., connecting several iMTI models in series, parallel or feedback loops results in another iMTI model. Applications of multilinear modelling in power systems are shown in [10, 11, 5]. This deliverable combines these three approaches by presenting the hybrid iMTI modelling class for power systems, though hybrid MTI models are a superclass of MTI models which are not restricted to

these cases only. A comprehensive review on hybrid (explicit and implicit) MTI modelling in different application domains is given in [12].

This document is organized as follows, chapter 2 introduces the fundamentals of hybrid implicit multilinear functions, chapter 3 presents tensor decomposition methods for hybrid iMTI models, chapter 4 introduces normalized hybrid iMTI models, chapter 5 shows application examples of hybrid iMTI models in power systems, and chapter 6 draws conclusions.

2 Hybrid implicit multilinear functions

Assume we have a model with $n \in \mathbb{N}$ continuous-valued state variables, $m \in \mathbb{N}$ continuous-valued input variables, $p \in \mathbb{N}$ continuous-valued algebraic variables, and $q \in \mathbb{N}$ binary-valued algebraic variables. First we start with then definition of hybrid implicit multilinear functions before deriving the model notation. Let the signal space of a hybrid implicit multilinear function be given by

$$\mathbf{v} = \begin{pmatrix} \delta\mathbf{x} \\ \mathbf{x} \\ \mathbf{u} \\ \mathbf{y} \\ \mathbf{z} \end{pmatrix} \in \mathbb{R}^n \times \mathbb{R}^n \times \mathbb{R}^m \times \mathbb{R}^p \times \mathbb{B}^q \equiv \mathbb{H}^{N_\mathbf{v}}, \tag{2.1}$$

with continuous-valued state vector $\mathbf{x} \in \mathbb{R}^n$, where $\delta\mathbf{x} \in \mathbb{R}^n$ stands for either the continuous-valued state derivate vector $\dot{\mathbf{x}}$ or the continuous-valued state transition vector $\mathbf{x}(k+1)$ with time instance variable $k \in \mathbb{Z}$ for continuous or discrete time respectively; with continuous-valued input vector $\mathbf{u} \in \mathbb{R}^m$, continuous-valued algebraic signal vector $\mathbf{y} \in \mathbb{R}^p$, and binary-valued algebraic signal vector $\mathbf{z} \in \mathbb{B}^q$; where $\mathbb{H}$ is a hybrid space that allows for a mix of real $\mathbb{R}$ and boolean $\mathbb{B}$ spaces with $N_\mathbf{v}$ hybrid variables [13].

A hybrid multilinear function $h : \mathbb{H}^n \to \mathbb{R}$ maps a hybrid space to a real number, which leads to the same result as a corresponding continuous-valued implicit multilinear function $h_c : \mathbb{R}^n \to \mathbb{R}$ if the binary variables are converted with the standard injector

$$\tilde{v}_l = \begin{cases} 1 \in \mathbb{R} & \text{if } v_l = \texttt{TRUE} \in \mathbb{B} \\ 0 \in \mathbb{R} & \text{if } v_l = \texttt{FALSE} \in \mathbb{B} \\ v_l & \text{if } v_l \in \mathbb{R}. \end{cases} \tag{2.2}$$

Furthermore, a hybrid multilinear vector function is a function $\mathbf{h} : \mathbb{H}^n \to \mathbb{R}^q$ that maps a hybrid space to a real vector space where each element is given by a hybrid multilinear function [13].

Thus, a hybrid implicit multilinear model can be represented by the set of inequality constrained difference- or differential-algebraic equations (d/DAEs)

$$\mathbf{0} = \mathbf{h}(\mathbf{v}), \tag{2.3}$$

$$\mathbf{0} \geq \mathbf{w}(\mathbf{v}), \tag{2.4}$$

where $\mathbf{h} : \mathbb{H}^{N_\mathbf{v}} \to \mathbb{R}^{N_H}$ and $\mathbf{w} : \mathbb{H}^{N_\mathbf{v}} \to \mathbb{R}^{N_W}$ are hybrid multilinear vector functions [13].

3 Decomposition

3.1 Tensors

Real-valued tensors $\mathsf{X} \in \mathbb{R}^{I_1 \times I_2 \times \cdots \times I_j}$ are multidimensional arrays that generalize matrices to higher dimensions, where j denotes the order of the tensor and I_k represents the size of the k-th mode. Well established linear control engineering methods mostly rely on matrices, i.e. two-dimensional tensors. However, for multilinear models, matrices are less appropriate parameter formats than general tensors due to the intrinsic tensor structure of multilinear monomials.

First, the monomial tensor is introduced, where the elements of the monomial tensor are given by [3]

$$\mathsf{M}(\mathbf{i}) = \prod_{j=1}^{n} x_j^{i_j - 1} \tag{3.1}$$

where $\mathbf{i} \in \{1, 2\}^n$ is the index vector.

Example 3.1. Consider a third-order system. Using (3.1), the element x_1 for example is denoted by $\mathsf{M}(2, 1, 1) = x_1$, or $\mathsf{M}(2, 2, 1) = x_1 x_2$. Continuing for the remaining elements leads to the following three-dimensional monomial tensor, depicted in Figure 3.1.
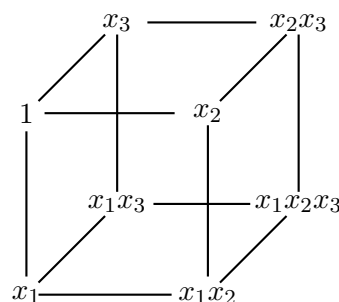

Figure 3.1: Monomial tensor for a third-order system, [3].

The contracted product $\langle \cdot | \cdot \rangle$ of tensors $\mathsf{F} \in \mathbb{R}^{I_1 \times \cdots \times I_n \times J_1 \cdots \times J_m}$ and $\mathsf{G} \in \mathbb{R}^{I_1 \times \cdots \times I_n}$ is defined as a

tensor $\mathsf{H} = \langle\, \mathsf{F} \mid \mathsf{G}\,\rangle \in \mathbb{R}^{J_1 \times \cdots \times J_m}$ with elements

$$H(j_1, \ldots, j_m) = \sum_{i_1=1}^{I_1} \sum_{i_2=1}^{I_2} \cdots \sum_{i_n=1}^{I_n} g(i_1, \ldots, i_n) f(i_1, \ldots, i_n, j_1, \ldots, j_m)\ . \tag{3.2}$$

The contracted product for tensors of the same size is called inner (or element-wise) product, which can be used to define a multilinear function as

$$f(\mathbf{x}) = \langle\, \mathsf{F} \mid \mathsf{M}(\mathbf{x})\,\rangle \in \mathbb{R}\ , \tag{3.3}$$

with $\mathbf{x} \in \mathbb{R}^n$, represented by the inner (element-wise) product of a parameter tensor $\mathsf{F} \in \mathbb{R}^{\times^n 2}$, using the tensor spaces notation

$$\mathbb{R}^{\times^{(n+m)}2} := \mathbb{R}^{\overbrace{2 \times \ldots \times 2}^{n+m}}\ ,$$

with the monomial tensor $\mathsf{M}(\mathbf{x})$ of the same dimension, [2, 3].

3.2 Decomposition of real tensors

The representation of the coefficients of a multilinear polynomial as tensor H as in (3.3) enables the application of tensor decomposition methods which have proven to be extremely powerful in many other application domains, [14]. This work focusses on the canonical polyadic (CP) decomposition.

A tensor X can be decomposed in a sum of R outer products. All the tensor X factors can be represented as matrices $\mathbf{F}_i \in \mathbb{R}^{I_i \times R_F}$ for each dimension i, [2], given as

$$\mathsf{X} = [\mathbf{F}_1, \mathbf{F}_2, \cdots, \mathbf{F}_n]\ . \tag{3.4}$$

An element of X is then given by

$$x(i_1, i_2, \ldots, i_n) = \sum_{j=1}^{R_F} \mathbf{F}_1(i_1, j) \cdot \mathbf{F}_2(i_2, j) \cdots \mathbf{F}_n(i_n, j)\ . \tag{3.5}$$

Figure 3.2 shows how the red element $x(3, 1, 2)$ of the tensor is computed as

$$F_1(3,1)F_2(1,1)F_3(2,1) + F_1(3,2)F_2(1,2)F_3(2,2) + \cdots + F_1(3,R_F)F_2(1,R_F)F_3(2,R_F)$$

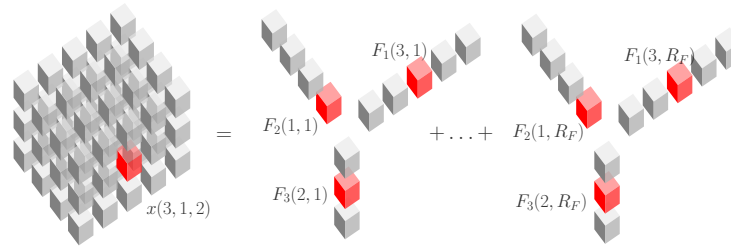by $R_F \cdot (n-1)$ multiplications and $(R_F - 1)$ summations.

Figure 3.2: CP Decomposition of a tensor with dimensions $5 \times 3 \times 4$, [3].

For engineering applications, finding an approximation of a given tensor F using a CP decomposition of a predefined rank can enable efficient representation. Minimizing the norm $\langle\, \mathsf{E}\, |\, \mathsf{E}\,\rangle$ of the error tensor

$$\mathsf{E}=\mathsf{F} - [\mathbf{F}_1, \cdots, \mathbf{F}_n] \tag{3.6}$$

is a non-convex hard problem. However, suboptimal solutions can be computed by tools like *Tensorlab* [15] for approximation in applications like the one given in this work in chapter 5.

3.3 Hybrid implicit CP models

The injector (2.2) in chapter 2 provides a transformation of Boolean variables into the real signal space. This approach will be used in the following, to write the hybrid iMTI model as a CP-decomposed tensor using the contracted product, where the tensor has been defined in the real space. As a result, the domain of the hybrid implicit multilinear function (2.3) will change from $\mathbb{H}^{N_\mathbf{v}}$ to $\mathbb{R}^{N_\mathbf{v}}$. Thus, using the injector (2.2) leads to an equivalent implicit multilinear function $\mathbf{h} : \mathbb{R}^{N_\mathbf{v}} \to \mathbb{R}^{N_\mathbf{v}}$.

Hybrid iMTI models can be presented as contracted tensor, where (2.3), and (2.4) can be represented by

$$\mathbf{0} = \langle\, \mathsf{H}\, |\, \mathsf{M}(\mathbf{v})\,\rangle\,, \tag{3.7}$$

$$\mathbf{0} \geq \langle\, \mathsf{W}\, |\, \mathsf{M}(\mathbf{v})\,\rangle\,, \tag{3.8}$$

with $\mathsf{H} \in \mathbb{R}^{\overbrace{2 \times \dots \times 2}^{N_\mathbf{v}} \times N_H}$ representing the equations' parameter tensor and

$$\mathsf{M}(\mathbf{v}) = \begin{pmatrix} 1 \\ v_{N_\mathbf{v}} \end{pmatrix} \circ \dots \circ \begin{pmatrix} 1 \\ v_1 \end{pmatrix} \in \mathbb{R}^{\overbrace{2 \times \dots \times 2}^{N_\mathbf{v}}}, \tag{3.9}$$

as the monomial tensor, which is constructed from the signal vector $\mathbf{v}$ using outer products

denoted by $\circ$; and $\mathsf{W} \in \mathbb{R}^{\overbrace{2 \times \cdots \times 2}^{N_{\mathbf{v}}} \times N_W}$ representing the parameter tensor associated with the inequality constraints, [9, 16].

After CP decomposition of the parameter tensors as well as the monomial tensor, the hybrid iMTI model reads as

$$0 = \left\langle \; [\mathbf{H}_1, \cdots, \mathbf{H}_{N_{\mathbf{v}}}, \mathbf{\Phi}_H] \; \middle| \; \left[\begin{pmatrix} 1 \\ v_1 \end{pmatrix}, \cdots, \begin{pmatrix} 1 \\ v_{N_{\mathbf{v}}} \end{pmatrix} \right] \; \right\rangle , \tag{3.10}$$

$$0 \geq \left\langle \; [\mathbf{W}_1, \cdots, \mathbf{W}_{N_{\mathbf{v}}}, \mathbf{\Phi}_W] \; \middle| \; \left[\begin{pmatrix} 1 \\ v_1 \end{pmatrix}, \cdots, \begin{pmatrix} 1 \\ v_{N_{\mathbf{v}}} \end{pmatrix} \right] \; \right\rangle , \tag{3.11}$$

with the structural factor matrices $\mathbf{H}_i \in \mathbb{R}^{2 \times R_H}$ and $\mathbf{W}_i \in \mathbb{R}^{2 \times R_W}$ for all hybrid signals $i = 1, \ldots, N_{\mathbf{v}}$, and parameter factor matrices $\mathbf{\Phi}_H \in \mathbb{R}^{N_H \times R_H}$ and $\mathbf{\Phi}_W \in \mathbb{R}^{N_W \times R_W}$.

If a CP decomposition of a parameter tensor is available, e.g., for H, the computation of the right-hand side of (3.7) is possible by using the factors and the rank-1 structure of the monomial tensor as

$$0 = \mathbf{\Phi}_H \left(\left(\mathbf{H}_1^\top \begin{pmatrix} 1 \\ v_1 \end{pmatrix} \right) \circledast \cdots \circledast \left(\mathbf{H}_{N_{\mathbf{v}}}^\top \begin{pmatrix} 1 \\ v_{N_{\mathbf{v}}} \end{pmatrix} \right) \right). \tag{3.12}$$

The total number of operations performed for each factor are $2R_H$ multiplications and $N_{\mathbf{v}}$ additions. Together with $N_{\mathbf{v}}$ multiplications for the element-wise Hadamard product $\circledast$ and the final multiplication with the $N_H \times R_H$ matrix $\mathbf{\Phi}_H$, these amount to a total of $(N_H + 2) R_H$ multiplications and $R_H + N_{\mathbf{v}}$ additions. This is linear in all dimensions $N_{\mathbf{v}}$ of the variables whereas already the number $2^{N_{\mathbf{v}}}$ of monomials has exponential complexity. Thus, full tensor computations are reasonable only for small dynamic order $2^{N_{\mathbf{v}}}$ of variables, whereas computations with decomposed representations are easily done up to very large dimensions, [3]. Similar arguments hold for the output (3.8).

4 Normalization

4.1 Normalization of signals

For normalization of each variable of the multilinear model given by

$$\tilde{v}_i = \frac{v_i - b_i}{a_i} \ \forall i = 1, \ldots, 2n + m + p + q \tag{4.1}$$

$$\tag{4.2}$$

the transformed equation matrix is given by

$$\widetilde{\mathsf{H}} = \operatorname*{diag}_{i=1,\ldots,2n+m+p+q} \left(\frac{1}{a_i} \right) (\mathbf{HT}) \tag{4.3}$$

where diag denotes the diagonal matrix with elements a_i and

$$\mathbf{T} = \begin{pmatrix} 1 & 0 \\ b_{2n+m+p+q} & a_{2n+m+p+q} \end{pmatrix} \otimes \cdots \otimes \begin{pmatrix} 1 & 0 \\ b_1 & a_1 \end{pmatrix}$$

is a transformation matrix, [17]. Linear transformations allow a numerical preconditioning of models and can also be done in tensor representation.

4.2 Hybrid implicit MTI models in CPN notation

As seen in section 3.3, given the exponential complexity of the model tensors H and W with the number of signals, factorizations are used for higher order models, e.g., CP tensor decompositions, [2].

For hybrid iMTI models, the parameter tensors in CP-decomposed format can be normalized using the absolute value norm to store it efficiently. For example, each factor matrix $\mathbf{H}_i \in \mathbb{R}^{2 \times R_H}$ of the parameter tensor H (except the last $\mathbf{H}$) can be normalized using the 1-norm (absolute

value norm) such that

$$||\widetilde{\mathbf{H}}_i(:,k)||_1 = \sum_{j=1}^{2} |\widetilde{\mathbf{H}}_i(j,k)| = |\widetilde{\mathbf{H}}_i(1,k)| + |\widetilde{\mathbf{H}}_i(2,k)| = 1 \,. \tag{4.4}$$

where the entries of the normalized factor matrix $\widetilde{\mathbf{H}}_i \in \mathbb{R}^{2 \times R_H}$ are

$$\widetilde{\mathbf{H}}_i = \begin{pmatrix} \mathbf{1} - ||\widetilde{\mathbf{h}}_i||_1^{\circledast} \\ \widetilde{\mathbf{h}}_i \end{pmatrix} \,, \tag{4.5}$$

where $||.||_1^{\circledast}$ is the element-wise 1-norm (absolute value) operator, and

$$\widetilde{\mathbf{h}}_i(k) = \frac{\mathbf{H}_i(2,k)}{||\mathbf{H}_i(:,k)||_1} \cdot (2\sigma(\mathbf{H}_i(1,k)) - 1) \tag{4.6}$$

for all columns $k = 1 \ldots R_H$, is a single parameter row vector $\widetilde{\mathbf{h}}_i \in \mathbb{R}^{1 \times R_H}$, with σ Heaviside function

$$\sigma(x) = \begin{cases} 1 & \text{if } x \geq 0 \,, \\ 0 & \text{otherwise} \,. \end{cases} \tag{4.7}$$

From $\widetilde{\mathbf{h}}_i$, both rows of $\widetilde{\mathbf{H}}_i$ can be reconstructed as in (4.5); therefore making it a sufficient and compact representation of the factor matrix $\mathbf{H}_i$. Furthermore, stacking each single parameter row vector $\widetilde{\mathbf{h}}_i$ into a single structure matrix $\mathbf{S}_H \in \mathbb{R}^{N_{\mathbf{v}} \times R_H}$ as

$$\mathbf{S}_H = \begin{pmatrix} \widetilde{\mathbf{h}}_1 \\ \vdots \\ \widetilde{\mathbf{h}}_{N_{\mathbf{v}}} \end{pmatrix} \,, \tag{4.8}$$

can achieve a sufficient compact representation of the whole tensor H together with the original parameter matrix $\mathbf{\Phi}_H \in \mathbb{R}^{N_H \times R_H}$. The same can be defined for W as $\mathbf{S}_W \in \mathbb{R}^{N_{\mathbf{v}} \times R_W}$ along the parameter matrix $\mathbf{\Phi}_W \in \mathbb{R}^{N_W \times R_W}$, as described in [18], such that

$$h_j(\mathbf{v}) = \sum_{k=1}^{R_H} \mathbf{\Phi}_{H_{jk}} \prod_{i=1}^{N_{\mathbf{v}}} (1 - | s_{H_{ik}} | + s_{H_{ik}} v_i(k)) \,, \tag{4.9}$$

$$w_j(\mathbf{v}) = \sum_{k=1}^{R_W} \mathbf{\Phi}_{W_{jk}} \prod_{i=1}^{N_{\mathbf{v}}} (1 - | s_{W_{ik}} | + s_{W_{ik}} v_i(k)) \,, \tag{4.10}$$

for all rows $j = 1 \ldots N_H$ for H and $j = 1 \ldots N_W$ for W respectively, [16].

Example 4.1. Consider the simple continuous-time hybrid iMTI system

$$0 = 3\dot{x}_1 y_1 + 2z_1 x_1 - u_1 x_1 - u_1 z_1 x_1 + 2x_1, \tag{4.11}$$

$$0 = \dot{x}_1 - y_1, \tag{4.12}$$

$$0 \geq 5 - 5z_1 - x_1 + x_1 z_1, \tag{4.13}$$

with hybrid signal vector $\mathbf{v} = \begin{pmatrix} \dot{x}_1 & x_1 & u_1 & y_1 & z_1 \end{pmatrix}^{\top}$, where x_1 is a state with derivative $\dot{x}_1$, u_1 is an input, y_1 is an algebraic variable, and z_1 is a boolean variable. The corresponding normalized hybrid iMTI model in CP-decomposed format is given by the matrices

$$\mathbf{S}_H = \begin{pmatrix} 1 & 0 & 0 & 0 & 0 & 1 & 0 \\ 0 & 1 & 1 & 1 & 1 & 0 & 0 \\ 0 & 0 & 1 & 1 & 0 & 0 & 0 \\ 1 & 0 & 0 & 0 & 0 & 0 & 1 \\ 0 & 1 & 0 & 1 & 0 & 0 & 0 \end{pmatrix}, \tag{4.14}$$

$$\Phi_F = \begin{pmatrix} 3 & 2 & -1 & -1 & 2 & 0 & 0 \\ 0 & 0 & 0 & 0 & 0 & 1 & -1 \end{pmatrix}, \tag{4.15}$$

for the equation tensor **H**, and

$$\mathbf{S}_W = \begin{pmatrix} 0 & 0 & 0 & 0 \\ 0 & 0 & 1 & 1 \\ 0 & 0 & 0 & 0 \\ 0 & 0 & 0 & 0 \\ 0 & 1 & 0 & 1 \end{pmatrix}, \tag{4.16}$$

$$\Phi_W = \begin{pmatrix} 5 & -5 & -1 & 1 \end{pmatrix}, \tag{4.17}$$

for the inequality tensor **W**.

However, (4.11) and (4.13) can be further simplified by factorization leading to a more compact representation as

$$0 = 3\dot{x}_1 y_1 + (1 + z_1)(2 - u_1) x_1, \tag{4.18}$$

$$0 = \dot{x}_1 - y_1, \tag{4.19}$$

$$0 \geq (5 - x_1)(1 - z_1). \tag{4.20}$$

Though this representation no longer follows the normalization condition in (4.4). Therefore, it

needs to be normalized using (4.6) as

$$0 = 3\dot{x}_1 y_1 + 6 \left(\frac{1}{2} + \frac{1}{2} z_1 \right) \left(\frac{2}{3} - \frac{1}{3} u_1 \right) x_1, \tag{4.21}$$

$$0 = \dot{x}_1 - y_1, \tag{4.22}$$

$$0 \geq 12 \left(\frac{5}{6} - \frac{1}{6} x_1 \right) \left(\frac{1}{2} - \frac{1}{2} z_1 \right), \tag{4.23}$$

leading to the new structure and parameter matrices

$$\mathbf{S}_H = \begin{pmatrix} 1 & 0 & 1 & 0 \\ 0 & 1 & 0 & 0 \\ 0 & -\frac{1}{3} & 0 & 0 \\ 1 & 0 & 0 & 1 \\ 0 & \frac{1}{2} & 0 & 0 \end{pmatrix}, \tag{4.24}$$

$$\mathbf{\Phi}_H = \begin{pmatrix} 3 & 6 & 0 & 0 \\ 0 & 0 & 1 & -1 \end{pmatrix}, \tag{4.25}$$

for the equation tensor $\mathbf{H}$, and

$$\mathbf{S}_W = \begin{pmatrix} 0 \\ -\frac{1}{6} \\ 0 \\ 0 \\ -\frac{1}{2} \end{pmatrix}, \tag{4.26}$$

$$\mathbf{\Phi}_W = \begin{pmatrix} 12 \end{pmatrix}, \tag{4.27}$$

for the inequality tensor $\mathbf{W}$.

Remark. Note that the normalization using (4.6) is not reversible, as scaling factors can be distributed differently among the factors of the original system.

4.3 Minimal format

Model parameters for hybrid iMTI systems can be saved in binary format as proposed in [18]. For example, Figure 4.1 shows the structure of such a minimal representation for the tensor $\mathbf{H}$ of the hybrid iMTI system from Example 4.1, with respect to the structure and parameter matrices in (4.24) and (4.25).

In Figure 4.1, the first row of integers indicates the index of the variables, for $\{\dot{x}_1, x_1, u_1, y_1, z_1\}$

int16	0	-1	3	0	4	2	1	0	-1	0	3
float64	3.0	1.0	1.0	6.0	0.5	$-\frac{1}{3}$	1	0	1	-1	1

Figure 4.1: Structure of minimal representation for Example 4.1 tensor **H**.

the indices are $\{-1, 1, 2, 3, 4\}$, respectively. Note that the index 0 is reserved to mark the end of a summand with either a nonzero real factor which gives the corresponding element of the phi matrix or zero, indicating a new equation. In the case of a variable $\dot{x}_1$, being the derivative of x_1, it gets the negative of the index of x_1. The same would for $x_1 (k + 1)$ in the discrete time case. The second row contains the corresponding parameter values in double-precision floating-point format.

Current work is focused on the development of efficient routines for reading, writing, and combining such binary files, as well as for converting between this minimal format and the CP-decomposed tensor format presented in this report.

Remark. Note that the indices have to be unique. Therefore, when models are connected, the indices have to be transformed to ensure uniqueness.

5 Power systems application example

5.1 Phase-locked loop

A prominent component in power converters are phase-locked loops (PLLs), which are used to synchronize the power converter with grid voltage by estimating the phase angle and the grid frequency. The structure is shown Figure 5.1, where $\mathbf{v}_{abc} \in \mathbb{R}^3$ is the input three-phase voltage, $\mathbf{v}_{dq} \in \mathbb{R}^2$ is the voltage in the dq-rotating synchronous reference frame with the angular velocity $\omega \in \mathbb{R}$, and the phase angle $\theta \in \mathbb{R}$. The second-order model regulates the v_q component to zero to align v_d with a-component. The PLL uses the Park transformation, which utilizes trigonometric functions.

Using trigonometric identities, we can derive the following continuous-time, time-invariant second-order model of the PLL

$$\dot{\theta} = x_{\mathrm{I}} + k_{\mathrm{p}} \frac{1}{3} \left((-2v_{\mathrm{a}} + v_{\mathrm{b}} + v_{\mathrm{c}}) \sin(\theta) + \sqrt{3} (v_{\mathrm{b}} - v_{\mathrm{c}}) \cos(\theta) \right) + \omega_0, \tag{5.1a}$$

$$\dot{x}_{\mathrm{I}} = k_{\mathrm{i}} \frac{1}{3} \left((-2v_{\mathrm{a}} + v_{\mathrm{b}} + v_{\mathrm{c}}) \sin(\theta) + \sqrt{3} (v_{\mathrm{b}} - v_{\mathrm{c}}) \cos(\theta) \right), \tag{5.1b}$$

where x_{I} is the state of the first integrator in the PI-controller, k_{p} and k_{I} are the corresponding gain values, θ is the estimated angle given by the second integrator Note that the nominal angular grid frequency ω_0 is added in (5.1a).

Motivated by the work [19, 20], we introduce the following nonlinear change of variables [5]

$$x_1 = \cos(\theta), \tag{5.2a}$$
$$x_2 = \sin(\theta), \tag{5.2b}$$
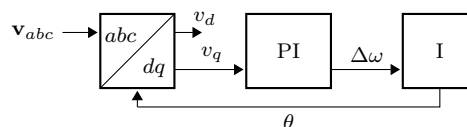$$x_3 = x_{\mathrm{I}}, \tag{5.2c}$$

Figure 5.1: Block diagram of a PLL

and the algebraic constraint

$$x_1^2 + x_2^2 = 1 \,. \tag{5.3}$$

Derivating (5.2) and inserting (5.1) into it leads to the iMTI model of (5.1) as

$$0 = \dot{x}_1 - \left(x_3 + k_\mathrm{p} \frac{1}{3} \left((-2u_1 + u_2 + u_3)\,x_2 + \sqrt{3}\,(u_2 - u_3)\,x_1 \right) + \omega_0 \right) (-y_2)\,, \tag{5.4a}$$

$$0 = \dot{x}_2 - \left(x_3 + k_\mathrm{p} \frac{1}{3} \left((-2u_1 + u_2 + u_3)\,x_2 + \sqrt{3}\,(u_2 - u_3)\,x_1 \right) + \omega_0 \right) (y_1) \tag{5.4b}$$

$$0 = \dot{x}_3 - k_\mathrm{I} \frac{1}{3} \left((-2u_1 + u_2 + u_3)\,x_2 + \sqrt{3}\,(u_2 - u_3)\,x_1 \right)\,, \tag{5.4c}$$

$$0 = x_1 - y_1\,, \tag{5.4d}$$

$$0 = x_2 - y_2\,, \tag{5.4e}$$

where y_1, y_2 are auxiliary algebraic variables to avoid having squares of the variables, which would be polynomial, but not multilinear. The three-phase voltages are the inputs $\mathbf{u} \in \mathbb{R}^3$. The multilinear system of differential-algebraic equations (5.4) square without the algebraic constraint (5.3). The algebraic constraint (5.3) is used to find consistent initial conditions for the system of differential-algebraic equations.

The nonlinear and iMTI model of the PLL are simulated in Matlab using the MTI Toolbox 2.1 [21]. Figure 5.2 shows that multilinear and nonlinear model show the same dynamic response to a disturbance in the grid frequency.
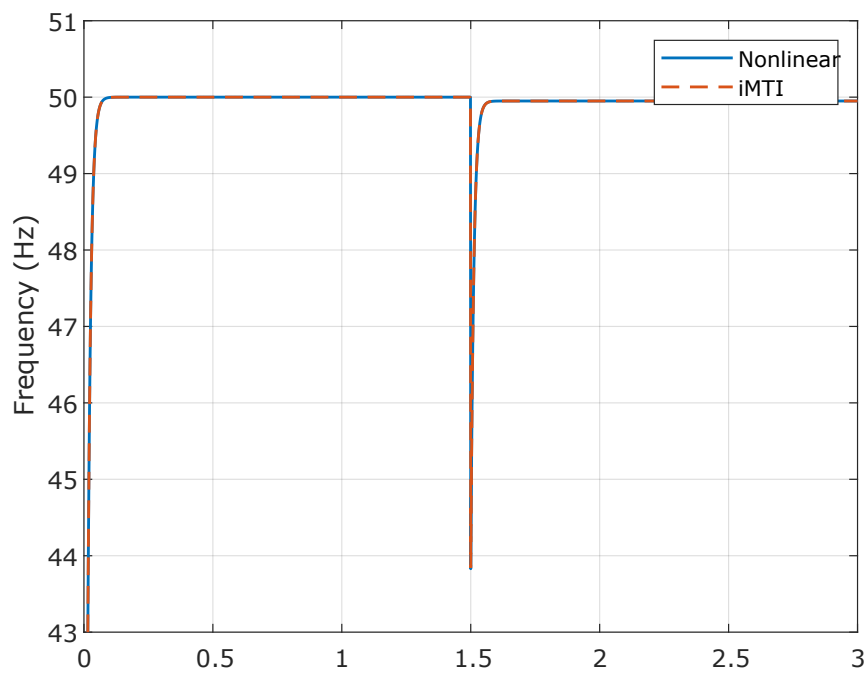
Figure 5.2: Simulation results of the nonlinear and iMTI model of the PLL

5.2 Converter control with saturation

The power electronics have a maximum current rating, and therefore, power converters need to limit their current output. Using a saturation for the reference value of the current is one possibility, where the upper and lower limit are typically $\pm 1.2\, \mathbf{i}_{dq,\text{rated}}$ of the rated current.

The hybrid iMTI model allows to represent saturation as follows

$$0 = y - u(1 - z_1)(1 - z_2) + u_{\text{lim,up}} z_1 - u_{\text{lim,low}} z_2 \tag{5.5a}$$

$$0 \geq (u_{\text{lim,up}} - u)(2z_1 - 1) \tag{5.5b}$$

$$0 \geq (u - u_{\text{lim,low}})(2z_2 - 1) \tag{5.5c}$$

where the upper and lower limit are $u_{\text{lim,up}}$, and $u_{\text{lim,low}}$, respectively, for an input variable u, the Boolean variables are $\mathbf{z} \in \mathbb{B}^2$, and y is the output. When the upper bound is applied, $z_1 = 1$, and when the lower bound is applied, $z_2 = 1$. For the hybrid iMTI model we get the following truth table shown in Table 5.1, where the first two columns show the inequalities.

Table 5.1: Truth table to model the saturation (5.5)

$u_{\text{lim,up}} - u$	$u - u_{\text{lim,low}}$	z_1	z_2	y
< 0	> 0	1	0	$u_{\text{lim,up}}$
≤ 0	≤ 0	0	0	u
> 0	< 0	0	1	$u_{\text{lim,low}}$

The model of an essential system consisting of a grid-following, and a grid-forming converter, presented in [5], was used, and a saturation was added using (5.5) in the current reference of the d-component in the grid-following converter. The obtained model was simulated using the MTI Toolbox [21] and the results are shown Figure 5.3. The upper plot shows the normalized reference current. At $2\,\text{s}$, the current reference rises but reaches the upper limit. The lower plot reflects what was expected from Table 5.1 that z switches from 0 to 1 to fulfill the inequality constraint (5.5b).
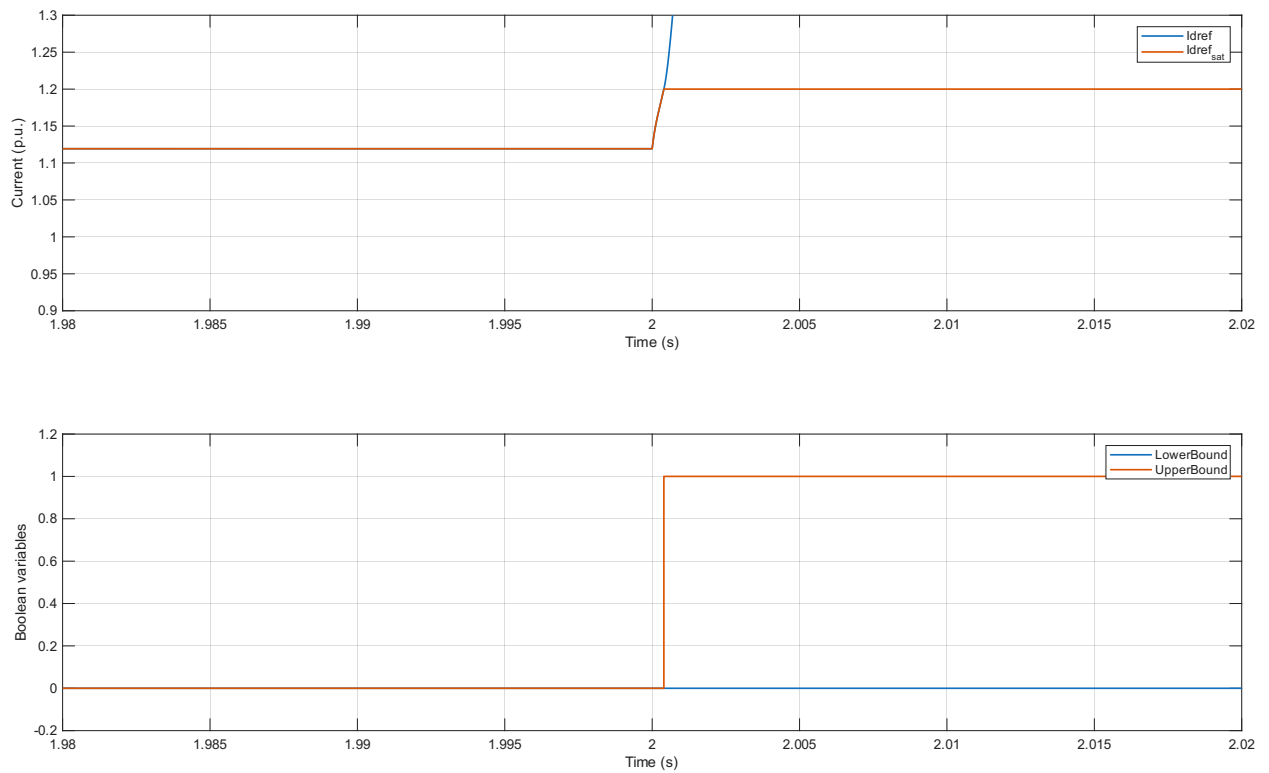
Figure 5.3: Simulation results of the saturation for i_d

6 Conclusion

This deliverable presents the hybrid implicit multilinear modeling class. It addresses the needs to the model class defined in Deliverable 3.1 [6].

Hybrid implicit multilinear models can represent complex dynamics that are encountered in power systems. The inclusion of Boolean variables allows representing discrete dynamics like saturations as it was shown in section 5.2. For some nonlinear functions, for example, trigonometric functions, section 5.1 shows that choosing a suitable change of variable, the nonlinear model can be represented in a different coordinate system where it is multilinear. In [5], it was shown that these are equivalent representation. Furthermore, power systems also encounter multilinear functions, for example in the calculation of power, or the current control as shown in [5].

Using the decomposed tensor format allows breaking the curse of dimensionality. The representation of iMTI models as canonical polyadic norm-1 (CPN1) decomposed was shown, which allows constructing a minimal format suitable for, e.g., model exchange.

Hybrid iMTI models of power systems, as well as other systems, can use the latest MTI Toolbox 2.1 release [21] in Matlab, where several examples are available.

Bibliography

[1] Georg Pangalos, Annika Eichler, and Gerwald Lichtenberg. *Tensor systems: multilinear modeling and applications*. 2013. DOI: `10.15480/882.2979`. URL: `http://hdl.handle.net/11420/5869`.

[2] Tamara G. Kolda and Brett W. Bader. "Tensor Decompositions and Applications". In: *SIAM Review* 51.3 (2009), pp. 455–500. DOI: `10.1137/07070111X`. eprint: `https://doi.org/10.1137/07070111X`. URL: `https://doi.org/10.1137/07070111X`.

[3] Gerwald Lichtenberg et al. "Implicit multilinear modeling: An introduction with application to energy systems". In: *at - Automatisierungstechnik* 70.1 (2022), pp. 13–30. DOI: `doi:10.1515/auto-2021-0133`. URL: `https://doi.org/10.1515/auto-2021-0133`.

[4] Gerwald Lichtenberg and Annika Eichler. "Multilinear Algebraic Boolean Modelling with Tensor Decompositions Techniques". In: *IFAC Proceedings Volumes* 44.1 (2011). 18th IFAC World Congress, pp. 5603–5608. ISSN: 1474-6670. DOI: `https://doi.org/10.3182/20110828-6-IT-1002.03612`. URL: `https://www.sciencedirect.com/science/article/pii/S147466701644499X`.

[5] Christoph Kaufmann et al. *Small-Signal Stability Analysis of Power Systems by Implicit Multilinear Models*. 2025. arXiv: `2510.16534 [eess.SY]`. URL: `https://arxiv.org/abs/2510.16534`.

[6] Pablo de Juan Vela and Josep Fanals i Batllori. *D 3.1 Report on Identified Non-linearities and Saturations*. TenSyGrid deliverable 3.1. eRoots, May 2025. URL: `https://tensygrid.eu/wp-content/uploads/2025/06/D3.1-Non-linearities-and-saturations_final_ERoots.pdf`.

[7] Teresa Wong and Gerwald Lichtenberg. *D 2.1 Improved Multilinearization Algorithm*. TenSyGrid deliverable 2.1. HAW, Nov. 2025.

[8] Pablo de Juan Vela et al. *D 3.2 Generation Multilinear Models and Validation*. TenSyGrid deliverable 3.2. eRoots, Nov. 2025.

[9] Georg Pangalos, Annika Eichler, and Gerwald Lichtenberg. "Hybrid Multilinear Modeling and Applications". In: *Simulation and Modeling Methodologies, Technologies and Applications*. Ed. by Mohammad S. Obaidat et al. Cham: Springer International Publishing, 2015, pp. 71–85. ISBN: 978-3-319-11457-6.

[10] Christoph Kaufmann et al. *Semi-explicit multilinear modeling of a PQ open-loop controlled PV inverter in ▨▨-frame*. en. 2023. DOI: `10.1016/j.egyr.2022.12.135`. URL: `https://publica.fraunhofer.de/handle/publica/448825`.

[11] Leandro Samaniego et al. "An Approach to Multi-Energy Network Modeling by Multilinear Models". In: *2024 European Control Conference (ECC)*. 2024, pp. 1522–1527. DOI: `10.23919/ECC64448.2024.10590975`.

[12]   Torben Warnecke et al. *Review on hybrid multilinear modelling and its applications*. submitted to Nonlinear Analysis: Hybrid Systems.

[13]   Torben Warnecke and Gerwald Lichtenberg. "Approach for the Mode Switching Problem in Piecewise Smooth Implicit Multilinear IVPs". In: *Proceedings of the 15th International Conference on Simulation and Modeling Methodologies, Technologies and Applications - Volume 1: SIMULTECH*. INSTICC. SciTePress, 2025, pp. 349–356. ISBN: 978-989-758-759-7. DOI: `10.5220/0013578200003970`.

[14]   Grey Ballard and Tamara G. Kolda. *Tensor Decompositions for Data Science*. Cambridge University Press, 2025.

[15]   N. Vervliet et al. *Tensorlab 3.0*. Available at `https://www.tensorlab.net`. Mar. 2016. URL: `https://www.tensorlab.net`.

[16]   Torben Warnecke and Gerwald Lichtenberg. "Hybrid implicit multilinear simulation using difference algebraic equations reordering by sparsity patterns*". In: *2024 10th International Conference on Control, Decision and Information Technologies (CoDIT)*. 2024, pp. 2578–2583. DOI: `10.1109/CoDIT62066.2024.10708218`.

[17]   Kai Kruppa, Georg Pangalos, and Gerwald Lichtenberg. "Multilinear Approximation of Nonlinear State Space Models". In: *IFAC Proceedings Volumes* 47.3 (2014). 19th IFAC World Congress, pp. 9474–9479. ISSN: 1474-6670. DOI: `https://doi.org/10.3182/20140824-6-ZA-1003.00455`. URL: `https://www.sciencedirect.com/science/article/pii/S1474667016431113`.

[18]   Niklas Jöres et al. "Reduced CP Representation of Multilinear Models". In: *Proceedings of the 12th International Conference on Simulation and Modeling Methodologies, Technologies and Applications - SIMULTECH*. INSTICC. SciTePress, 2022, pp. 252–259. ISBN: 978-989-758-578-4. DOI: `10.5220/0011273100003274`.

[19]   Michael A. Savageau and Eberhard O. Voit. "Recasting nonlinear differential equations as S-systems: a canonical nonlinear form". In: *Math. Biosci.* 87.1 (1987), pp. 83–115. ISSN: 00255564. DOI: `10.1016/0025-5564(87)90035-6`.

[20]   Marian Anghel, Federico Milano, and Antonis Papachristodoulou. "Algorithmic Construction of Lyapunov Functions for Power System Stability Analysis". In: *IEEE Trans. Circuits Syst. I Regul. Pap.* 60.9 (2013), pp. 2533–2546. DOI: `10.1109/TCSI.2013.2246233`.

[21]   Lichtenberg et al. *MTI Toolbox 2.1*. Available at `https://www.mti.systems`. Oct. 2025. URL: `https://www.mti.systems`.